

# Time-Domain Analysis of TM Scattering from Conducting Cylinders Using a Hybrid Method

Tanmoy Roy, Tapan K. Sarkar, *Fellow, IEEE*, Antonije R. Djordjevic, and Magdalena Salazar-Palma, *Member, IEEE*

**Abstract**—In this paper, the finite-element method (FEM) is used to solve open-region problems utilizing the time-domain differential form of Maxwell's equations. The radiation boundary condition for the open-region problem is enforced through the time-domain Green's function as used in integral-equation methods, yet keeping the sparsity of the FEM matrices. In this paper, the proposed method is applied to the time-domain analysis of TM scattering from conducting cylinders. At each time step, the fields inside the discretized domain are calculated using the FEM. The computed induced currents of earlier time steps, together with contributions from the present time step, give the radiation condition at the terminating surface. Numerical results are presented to illustrate the applicability of this technique.

**Index Terms**—FEM method, hybrid techniques, time domain, TM scattering.

## I. INTRODUCTION

IN THIS paper, we solve the transient two-dimensional wave equation using a combination of the finite-element technique and the concept of the Green's function associated with an integral-equation approach. For the TM scattering problem, since  $E_z(x, y, t)$  is the axial  $z$ -component of the electric field, the wave equation in the time domain can be written as

$$\begin{aligned} \nabla^2 E_z(x, y, t) - \frac{1}{c^2} \frac{\partial^2 E_z(x, y, t)}{\partial t^2} \\ = \frac{\partial^2 E_z(x, y, t)}{\partial x^2} + \frac{\partial^2 E_z(x, y, t)}{\partial y^2} - \frac{1}{c^2} \frac{\partial^2 E_z(x, y, t)}{\partial t^2} \\ = 0, \quad x, y, \in R, \quad t \in (0, \infty). \end{aligned} \quad (1)$$

Here,  $R$  is the spatial domain of the problem,  $E_z$  is independent of  $z$ , and  $c$  is the velocity of the wave in the medium considered. Triangular finite elements are used to discretize the computational domain. In the finite-element method (FEM), the computational domain must be finite. Thus, an artificial boundary must be introduced to terminate it, and an

adequate radiation boundary condition should be imposed on the fictitious boundary. In this paper, the radiation condition is enforced in an exact way, utilizing the free-space time-domain Green's function arising from the integral-equation approach. This hybrid method has been used successfully for electrostatic [1] and frequency-domain solutions of Maxwell's equation [2]. In this paper, we extend the methodology for the solution of transient problems. The FEM used in this paper is node based. The field quantities are computed at each node, as opposed to staggered in space, as done for finite difference time domain (FDTD) [3].

Time-domain integral equations have been used in the past to solve for transient scattering problems. However, in some cases, the method exhibits late time instabilities, even though the Courant stability condition was satisfied [4]–[9]. Although some remedies have been suggested, the late time instability is still an open problem. An implicit scheme has been proposed to reduce such instabilities. Namely, Barkeshli *et al.* [10] have used the implicit Newmark method in the application of the boundary integral technique to solve for transient electromagnetic-field coupling to a metallic enclosure. Gedney and Navsariwala [11] have used the Newmark method in conjunction with the time-dependent vector wave equation. They showed that this procedure leads to a stable solution under certain values of some parameters.

In this paper, we utilize the Newmark method to solve the transient two-dimensional TM scattering for open-region problems utilizing the FEM and Green's function technique.

## II. FORMULATION

Consider a Gaussian pulse incident on a conducting structure, as shown in Fig. 1. The electric incident field is given by

$$\bar{E}_i = E_0 \frac{4}{T\sqrt{\pi}} e^{-\gamma^2 \hat{z}} \quad (2)$$

where  $\hat{z}$  is the unit vector along the  $z$ -direction, and  $T$  is the width of the Gaussian pulse.  $E_0$  is a constant and provides the initial amplitude of the Gaussian electric field. Here,  $\gamma$  is given by

$$\gamma = \frac{4}{T}(ct - ct_0 + x \cos \theta + y \sin \theta), \quad (3)$$

Equation (1) is satisfied by the incident electric field  $\bar{E}_i$ , scattered electric field  $\bar{E}_s$ , produced by the currents induced

Manuscript received August 29, 1996; revised April 21, 1998.

T. Roy was with the Department of Electrical Engineering and Computer Science, Syracuse University, Syracuse, NY 13244-1240 USA. He is now with Sun Microsystems, Palo Alto, CA 94303 USA.

T. K. Sarkar is with the Department of Electrical Engineering and Computer Science, Syracuse University, Syracuse, NY 13244-1240 USA (e-mail: tksarkar@mailbox.syr.edu).

A. R. Djordjevic is with the Department of Electrical Engineering, University of Belgrade, 11001 Belgrade, Yugoslavia.

M. Salazar-Palma is with the Departamento de Senales, Sistemas y Radio-Comunicaciones, ETSI Telecomunicacion, Universidad Politecnica de Madrid, Madrid 28040, Spain.

Publisher Item Identifier S 0018-9480(98)07240-8.

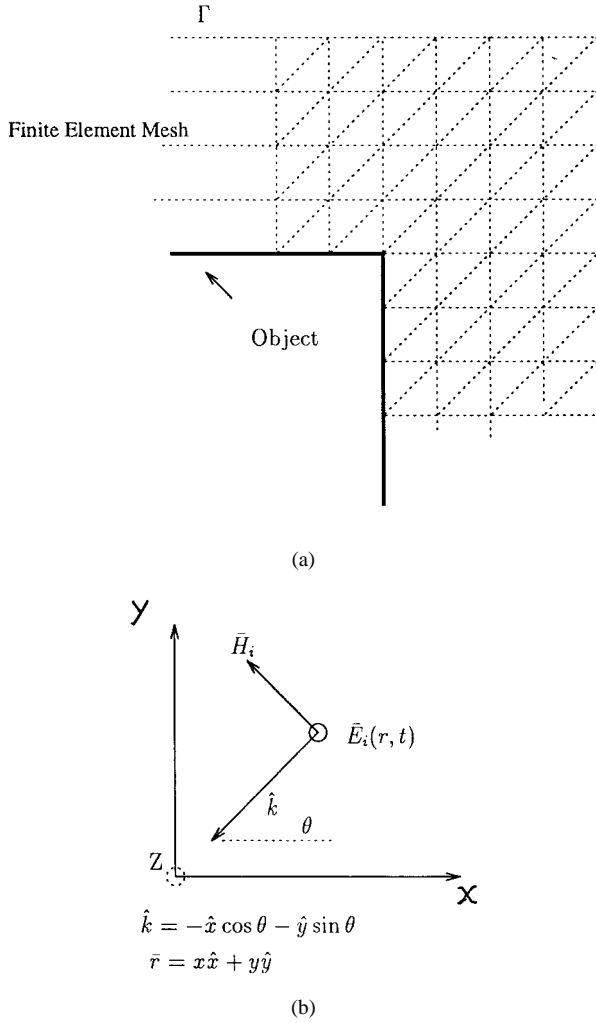


Fig. 1. Finite-element mesh for a body and the incident field.

on the conductor, and the total field, which is given as

$$\vec{E}(\vec{r}, t) = \vec{E}_i(\vec{r}, t) + \vec{E}_s(\vec{r}, t). \quad (4)$$

Here,  $\vec{r}$  is the position vector with respect to the origin. The scattered field  $\vec{E}_s$  is given by

$$\vec{E}_s(\vec{r}, t) = -\frac{\partial \vec{A}}{\partial t}$$

and using the backward difference at time  $t_n$ , it can be written as

$$\simeq -\frac{1.5\vec{A}(\vec{r}, t_n) - 2\vec{A}(\vec{r}, t_{n-1}) + 0.5\vec{A}(\vec{r}, t_{n-2})}{\Delta t} \quad (5)$$

where  $\vec{A}$  is the magnetic vector potential.

Due to the causal nature of the induced surface current, the magnetic vector potential at time instant  $t_n$  is given by [4], [5]

$$\vec{A}(r, t_n) = \frac{\mu C}{2\pi} \oint_C dr' \int_{t'=0}^{t_n - P/c} \frac{\vec{J}_s(\vec{r}', t') dt'}{\sqrt{c^2(t_n - t')^2 - P^2}} \quad (6)$$

where  $P$  is given by  $|\vec{r} - \vec{r}'|$  and  $\vec{r}'$  is the source position vector.

As the conductor surface is divided into a number of subsections in the process of the finite-element discretization,

the integral over the conductor surface can be broken into finite sums, consisting of lengths  $\Delta l_i$ , which can be given as

$$\vec{A}(r, t_n) = \frac{\mu C}{2\pi} \sum_i \int_{\Delta l_i} dr' \int_{t'=0}^{t_n - P/c} \frac{\vec{J}_{\Delta l_i}(\vec{r}', t') dt'}{\sqrt{c^2(t_n - t')^2 - P^2}}. \quad (7)$$

Since the cylindrical structure is perfectly conducting, the boundary condition requires the tangential component of the total electric field to be zero on the conductor. Since, for the TM case, the transverse electric field is identically zero, the boundary condition reduces to

$$E_z^{\text{tan}}(\vec{r}, t) = 0 \quad (8)$$

on the conductor surface. We can express the surface-current density on the conductor in terms of the tangential magnetic field just outside (the superscript +) the conductor. Hence, (8) leads us to

$$\vec{J}_s(\vec{r}, t) = \hat{n} \times \vec{H}_t^+(\vec{r}, t) \quad (9)$$

where  $\hat{n}$  is the unit normal on the conductor surface. The transverse component of the magnetic field is related to  $E_z$  through

$$\frac{\partial \vec{H}_t}{\partial t} = \frac{1}{\mu} \hat{z} \times \nabla_t E_z. \quad (10)$$

Now, computing the transverse magnetic fields at a time instant  $t_n$ , we have

$$H_x(\vec{r}, t_n) \simeq H_x(\vec{r}, t_{n-1}) + \frac{\Delta t}{\mu} \frac{dE_z(\vec{r}, t_n)}{dn}. \quad (11)$$

Similarly, we get

$$H_y(\vec{r}, t_n) \simeq H_y(\vec{r}, t_{n-1}) + \frac{\Delta t}{\mu} \frac{dE_z(\vec{r}, t_n)}{dn}. \quad (12)$$

Also, from (9), the induced currents on the conductor surface at time instant  $t_n$  can be given as

$$\vec{J}_s(\vec{r}, t_n) \simeq \vec{J}_s(\vec{r}, t_{n-1}) + \frac{\Delta t}{\mu} \frac{dE_z(\vec{r}, t_n)}{dn}. \quad (13)$$

For computing the time derivatives of the magnetic fields, we have used first-order approximations. One can employ higher order approximation, but with added cost of memory storage and computational complexity. Expression (13) allows one to compute the current distribution on the conductor surface at time instant  $t_n$  from the earlier time steps and normal derivative of the axial electric field at time instance  $t_n$ . Thus, once  $E_z$  is computed at time instance  $t_n$  through the application of the FEM, a simple postprocess will give its normal derivative and the updated current distribution.

### III. FINITE-ELEMENT PROCEDURE

In this section, we will use a variational formulation to transform the two-dimensional wave equation into a matrix equation. The open region surrounding the body is discretized into nonoverlapping finite elements. Since the domain of discretization must be finite, a fictitious boundary has been introduced to bound the computational domain only four layers

away from the object. Triangular finite elements are chosen for the ease of simulation of any arbitrary geometry. The meshing around the structure need not be conformal to the body, but the efficiency of the solution increases if we use body-fitting meshes in the solution procedure. To find the axial electric field  $E_z$  for the two-dimensional solution region, we seek an approximation for  $E_z^e$  within an element  $e$  and then interrelate the fields in the various elements such that the electric field  $E_z$  is continuous across interelement boundaries [12], [13]. Using a polynomial approximation of  $E_z$  over each element, the solution for the whole region is given by

$$E_z(x, y, t) \simeq \sum_{e=1}^N u^e(x, y) \psi^e(t) \quad (14)$$

where  $N$  is the number of triangular elements into which the bounded domain is divided. We will be using linear polynomial functions over an element for the variation for  $u^e(x, y)$ . A semidiscrete finite-element model is assumed for discretization purposes. The spatial approximation is considered first and the time approximation next.

For notational convenience, we will be using  $\phi$  instead of  $E_z$  in (8). Now, we seek a solution space  $V = \{v \in H^1(\mathcal{R}); v = u_0 \text{ a constant on } \Gamma\}$ , where  $H^1$  denotes the Hilbert space for this problem. Multiplying (1) with  $v$  and integrating over the domain  $\mathcal{R}$ , one gets the Galerkin formulation of the problem.  $\phi$  for a particular element  $e$  can be given as

$$\phi^e = \sum_{j=1}^3 \alpha_j(x, y) \phi_j^e(t) \quad (15)$$

where  $\alpha_j$ 's are the element-shape functions, as given in [12], and  $\phi_j^e(t)$  are the values of  $E_z$  at the element nodes at each time step. Substituting (15) into the Galerkin formulation, one gets from element  $e$  the expression

$$-\frac{1}{c^2} [T^e][\ddot{\phi}] = -[C^e][\phi] \quad (16a)$$

where the coefficients of  $[T^e]$  and  $[C^e]$  are

$$T_{ij} = \int_{\text{Re}} \alpha_i \alpha_j ds \quad (16b)$$

$$C_{ij} = \int_{\text{Re}} \left( \frac{\partial \alpha_i}{\partial x} \frac{\partial \alpha_j}{\partial x} + \frac{\partial \alpha_i}{\partial y} \frac{\partial \alpha_j}{\partial y} \right) ds \quad (16c)$$

and  $\text{Re}$  is the element domain.

Now, assembling all such elements in the solution region, an ordinary differential equation for the assemblage is given by

$$\frac{1}{c^2} [T][\ddot{\phi}] = -[C][\phi] \quad (17a)$$

and, alternately,

$$[B][\ddot{\phi}] = [A][\phi]. \quad (17b)$$

The matrices  $[C]$  and  $[T]$  are the assemblage of individual coefficient matrices  $[C^e]$  and  $[T^e]$ , respectively. It is evident that the  $[C]$  and  $[T]$  are time-independent matrices. We have replaced matrices  $\frac{1}{c^2}[T]$  and  $-[C]$  by  $[B]$  and  $[A]$ , respectively, for notational convenience. The column matrix  $[\phi]$  represents  $E_z(r, t)$  at the corresponding nodes.

#### IV. TIME-STEPPING PROCEDURE

Equation (17) is a system of a second-order differential equation, which will be solved by Newmark's method [10], [11]. For certain values of the parameter, the Newmark method is unconditionally stable and introduces the best truncation error for certain specific parameters. The algorithm starts by expanding  $\dot{\phi}$  (equivalent to matrix  $[\dot{\phi}]$ ) and  $\phi$  (equivalent to matrix  $[\phi]$ ) at time  $t_{n+1}$  as

$$\dot{\phi}_{t_{n+1}} = \dot{\phi}_{t_n} + [(1 - \delta)\ddot{\phi}_{t_n} + \delta\ddot{\phi}_{t_{n+1}}]\Delta t \quad (18a)$$

$$\phi_{t_{n+1}} = \phi_{t_n} + \dot{\phi}_{t_n}\Delta t + \left[ \left( \frac{1}{2} - \alpha \right) \ddot{\phi}_{t_n} + \alpha\ddot{\phi}_{t_{n+1}} \right] \Delta t^2 \quad (18b)$$

where  $\alpha$  and  $\delta$  are parameters that can be chosen to obtain accuracy and stability. Typically, the values for  $\alpha$  and  $\delta$  are 1/4 and 1/2, respectively. However, one can choose the parameters using  $\delta \geq 1/2$  and  $\sigma \geq 0.25(0.5 + \delta)^2$ .

Next we multiply (18a) and (18b) by  $B$  and use (17b) to obtain

$$[B]\dot{\phi}_{t_{n+1}} = [B]\dot{\phi}_{t_n} + \{(1 - \delta)[A]\phi_{t_n} + \delta[A]\phi_{t_{n+1}}\}\Delta t \quad (19a)$$

and

$$[B]\phi_{t_{n+1}} = [B]\phi_{t_n} + \Delta t[B]\dot{\phi}_{t_n} + \{(0.5 - \alpha)[A]\phi_{t_n} + \alpha[A]\phi_{t_{n+1}}\}\Delta t^2 \quad (19b)$$

writing (19b) for time instance  $t_{n+1}$  and subtracting (9b) from it and substituting  $\dot{\phi}_{t_{n+1}} - \dot{\phi}_{t_n}$  from (19a), one obtains a two-step recurrence relation for the wave equation. Now, replacing  $([B] - \Delta t^2 \alpha [A])$  by  $L$ ,  $-2[B] - \Delta t^2(0.5 + \delta - 2\alpha)[A]$  by  $[M]$ , and  $[B] - \Delta t^2(0.5 - \delta + \alpha)[A]$  by  $N$ , we can rewrite the above equation in a compact form as

$$L\phi_{t_{n+2}} + M\phi_{t_{n+1}} + N\phi_{t_n} = 0. \quad (20)$$

Equation (20) can be split into two parts for two types of nodes. The first set of nodes are called free nodes, on which the electric field needs to be solved for, and the second set are called fixed nodes, on which  $E_z(r, t)$  are known. If all the free nodes are numbered first and the fixed nodes last, we can rewrite (20) as

$$\begin{aligned} & \begin{bmatrix} L_{ff} & L_{fp} \\ L_{pf} & L_{pp} \end{bmatrix} \begin{bmatrix} \phi_f \\ \phi_p \end{bmatrix}^{n+2} \\ &= - \begin{bmatrix} M_{ff} & M_{fp} \\ M_{pf} & M_{pp} \end{bmatrix} \begin{bmatrix} \phi_f \\ \phi_p \end{bmatrix}^{n+1} - \begin{bmatrix} N_{ff} & N_{fp} \\ N_{pf} & N_{pp} \end{bmatrix} \begin{bmatrix} \phi_f \\ \phi_p \end{bmatrix}^n \end{aligned} \quad (21)$$

where subscripts  $f$  and  $p$  refer to free and fixed nodes, respectively. The superscript for matrices denotes the values at a particular time instant. As evident, the matrices  $[L]$ ,  $[M]$ , and  $[N]$  do not change at every time step. This equation similarly can be written in terms of the unknown vector  $[\phi_f]$  at time instant  $t_{n+2}$  in terms of previous time instances  $t_{n+1}$  and  $t_n$ .

To solve for the field quantities at time instant  $t_{n+2}$ , we will replace the values of  $[\phi_f]$  and  $[\phi_p]$  at time instants  $t_{n+1}$  and  $t_n$  either from the field values at previous time steps, boundary condition on the body, or radiation condition on the terminating surface. Suppose we know the field sources

within the mesh. These sources are the induced currents on the conductor surfaces. These sources produce a field in the free space, and the scattered field at the terminating surface can be evaluated at time  $t_n$  using (7) and (13). Hence, the magnetic vector potential at time  $t_n$  can be written as

$$\bar{A}(r, t_n) = \frac{\mu c}{2\pi} \Delta t \sum_i \sum_k \bar{J}_{\Delta 1_i}(l_i, k\Delta t) \int_{\Delta 1_i} \frac{dl'}{\sqrt{c^2(t_n - k\Delta t)^2 - P^2}}, \quad 0 \leq k\Delta t \leq t_n - P/c. \quad (22)$$

Equation (21) needs to be solved for computing the free-node values at time instant  $t_{n+2}$ . However, to start the two-step recurrence relation, we need to define the initial conditions for the free and fixed nodes. We assume that the Gaussian incident pulse is switched on at  $t = 0$  for all spaces surrounding the body, and the field values for the nodes for previous times are assumed to be identically zero before  $t \leq 0$ . Hence, we can use (21) to compute for the free nodes at time  $t = 0$ . Similarly, the values of the nodes for  $t = \Delta t$  can be found by using the same equation. Due to the causal nature of the time-domain problem, there has to be a finite amount of time that should elapse (namely,  $P/c$ ) before we can compute the effect of the induced current on the terminating surface.

The proposed method can be regarded as a hybrid of differential- and integral-equation techniques, because a finite-element approach is applied for the electric field within the domain, and a boundary condition expressed in terms of an integral (containing the unknown source distribution under the integral) is formulated for the terminating surface, which is given by the Green's function.

## V. NUMERICAL RESULTS

### A. Square Cylinder

Let us consider the case of a square cylinder of side 1.0 m, illuminated by a Gaussian pulse of unit amplitude ( $E_0 = 1$ ). The incident wave is traveling along the negative  $x$ -axis, i.e.,  $\theta = 0$ . We have used four layers of finite elements from the surface of the body. In this example, the fictitious surface is only 0.2 m away from the body. The terminating surface comprises of 80 nodes, whereas 48 fixed nodes form the conductor surface. The inner layer between the conductor and terminating surface consists of 192 free nodes. For the total field formulation, the tangential electric field on the conductor is zero.

The pulsewidth of the Gaussian pulse is taken to be  $T = 2.0$  LM. The delay of the pulse ( $t_0$ ) is given in terms of distance as 3.0 m ( $ct_0 = 3.0$  m). This means that the Gaussian pulse will reach its maximum at the origin at  $t_0 = \frac{3}{c}$  s. The time step ( $\Delta t$ ) for this example is chosen to be  $\frac{1}{21c}$ , where  $c$  is the velocity of the wave in free space. After turning on the Gaussian pulse at  $t = 0$ , we compute the fields for the free nodes and those on the terminating surface using (21). As the fields are known for that particular instant, the induced surface currents may be computed through (13) for that instant. Hence, the radiation condition on the terminating surface is applied

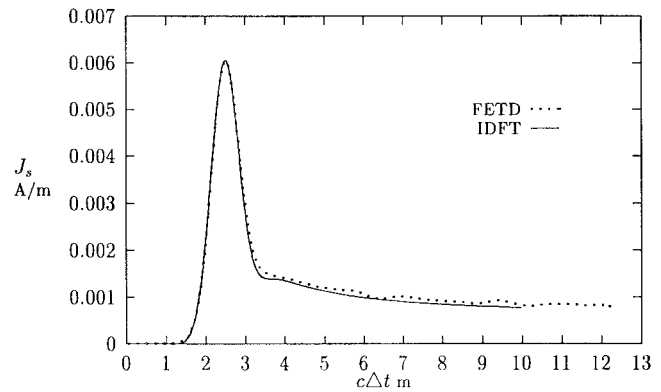


Fig. 2. Induced current on the square conductor at (0.5, 0.0). Outer boundary—0.2 m away.

through the Green's function integral. Now, the scattered field on the terminating surface is computed through (5). These values are replaced in (21) and the time-stepping procedure continues to compute fields for the next time step. In our analysis, to get integration accuracy and stability, we have used values of 0.25 and 0.5 for  $\alpha$  and  $\delta$ , respectively.

The induced surface-current distribution on the particular segment of the body is calculated as a postprocess from the computed longitudinal electric-field component following (12). The induced surface current on the conductor for a point on the  $x$ -axis (0.5, 0.0) is plotted in Fig. 2, with respect to  $c\Delta t$ , and is marked by finite-element time domain (FETD). As the peak of the incident pulse arrives, the front face of the square cylinder at  $\frac{2.5}{c}$  s. the induced surface current is maximum during that time. With the progression of time, the incident pulse moves toward the back of the conductor; hence, the induced current at the middle of the front face decreases. After the pulse crosses it completely, the current starts decaying slowly.

The result from this method is compared with the Fourier-transformed frequency-domain method-of-moments (MOM) results [14]. To produce these other results, we have used 48 subsections to calculate induced current on the conductor with the incident pulse being Gaussian, but frequency transformed. The pulse basis functions and point-matching testing procedure are used to evaluate the current on the conductor. We have chosen 256 equally spaced frequency points from zero to 0.5 GHz to produce the frequency-domain currents. These values are inverse discrete Fourier transformed (IDFT) to get time-domain results. This is marked as IDFT in Fig. 2. As can be seen from Fig. 2, the two results agree well.

In this example, we have employed total-field formulation. The total electric field on a node residing on the terminating surface is shown in Fig. 3, with respect to  $c\Delta t$ . This node lies on the  $x$ -axis, but just opposite to a node at the middle of the conductor. We can see that the pulse passes through this point and reaches its maximum around  $\frac{2.3}{c}$  s. However, the reflected pulse from the front face of the conductor, which is negative of the incident pulse, slowly arrives at the terminating surface. The negative pulse reaches its peak around  $t = \frac{3}{c}$  s.

Now, let us see how do the induced current on the surface of the conductor behaves in late time. Here, we have computed the induced current at the middle of the front face of the

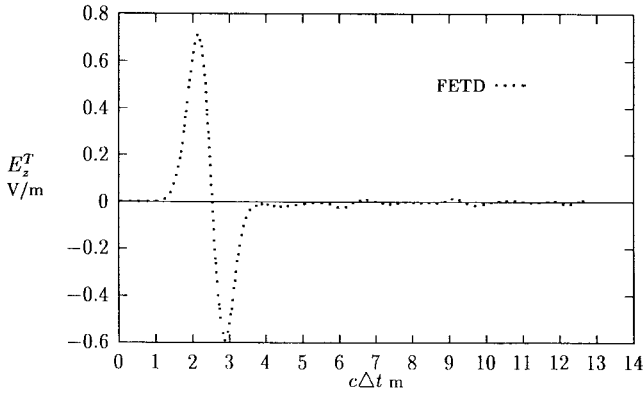


Fig. 3. Total electric field on the terminating surface at a point (0.7, 0.0).

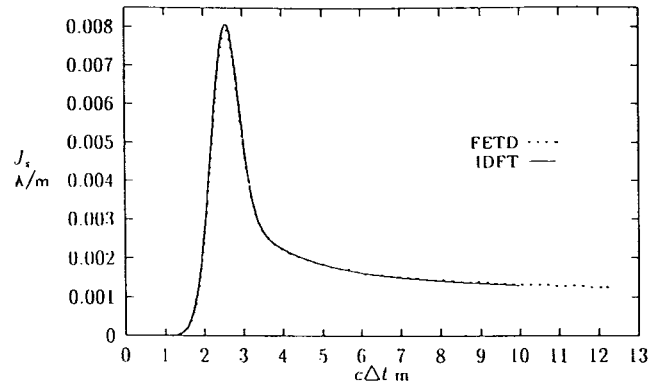


Fig. 5. Induced current on the circular conductor at (0.5, 0.0). Outer boundary—0.2 m away.

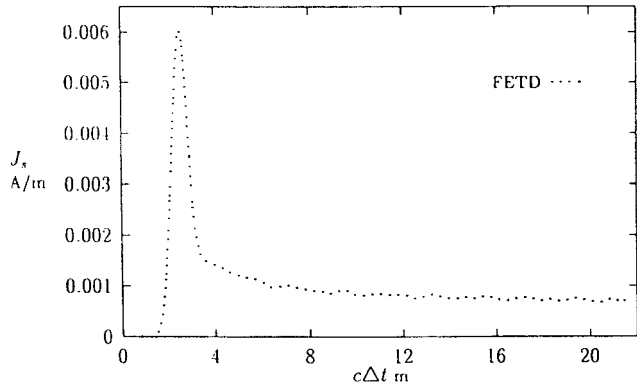


Fig. 4. Induced current on the square conductor at (0.5, 0.0). Outer boundary—0.2 m away.

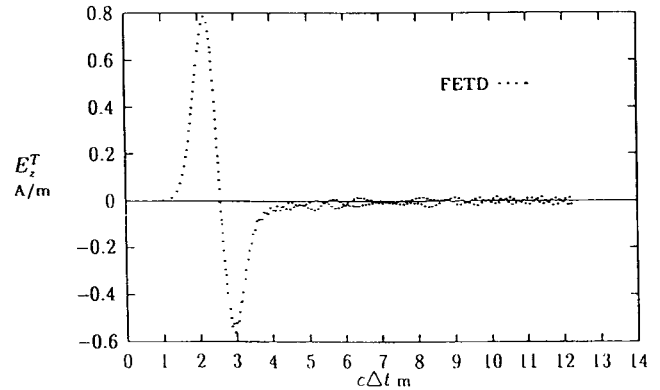


Fig. 6. Total electric field on the terminating surface at a point (0.7, 0.0).

conductor, illuminated by a Gaussian pulse. As we can see from Fig. 4, the induced current at late times does not show any instability or any kind of oscillations. Even though we can observe small ripples, they never grow beyond some values and die down slowly as the solution procedure progresses later.

**B. Circular Cylinder**

Let us consider the case of a circular cylinder of diameter 1.0 m. A four-layer finite-element mesh has been used for this problem. In this example, the terminating surface is 0.2 m away from the conductor surface. There are 88 fixed nodes, 44 of them are on the conductor surface and the other 44 are on the outside boundary or the terminating surface. Another 132 free nodes resides between the conductor and the terminating surface. They are coefficients of the unknown vector of the FEM system.

The incident field is a Gaussian pulse with  $T = 2.0$  LM and  $ct_0 = 3.0$  m. The wave is of unit amplitude ( $E_0 = 1$ ) and is coming from the positive  $x$ -direction. The coordinate axis is centered at the center of the cylinder. In this case, we have also used the total-field formulation. Hence, the time-stepping procedure starts by assuming  $\bar{E}_z$  on the outside boundary and zero field on the conductor surface for all times. We switch on the incident field at time  $t = 0$  all over the computational space. Equation (21) is solved at every time step for the free nodes to compute the electric field at those nodes. With these known values of the field in the computational domain,

we compute the normal derivative of the axial electric field for that time instant on the conductor. From it, the current distribution on a particular segment of the body is calculated through (13). Now, the scattered electric field is computed at the terminating surface at that instant using (5) and the known induced current on the conductor. After replacing the total electric field for the nodes at the terminating surface, we employ the recurrence relation to find the electric fields for the free nodes and compute the induced current distribution on the conductor for the next time step. In this context, we should mention that for an initial few time steps, the total electric field on the terminating surface is essentially the incident field, as the induced currents take finite time to travel from the source point to the field point to produce the scattered field.

The induced surface current on a node residing on the  $x$ -axis is plotted in Fig. 5, with respect to time. In this example, we have chosen a time step of  $\frac{1}{21c}$  s. As we can observe, the induced surface current reaches a maximum near about 2.51 LM ( $1$  LM = 3.335 64 ns) as the front face of the cylinder is getting illuminated by the peak of the Gaussian pulse. The results, marked as FETD, are compared with the inverse discrete Fourier-transformed frequency-domain MOM results marked as IDFT. We have used 256 equally spaced frequency points from zero to 0.5 GHz to produce the time response. As before, we have used pulse basis and point-matching testing procedure for frequency-domain results. For the MOM, 40 subsections are chosen on the conducting surfaces.

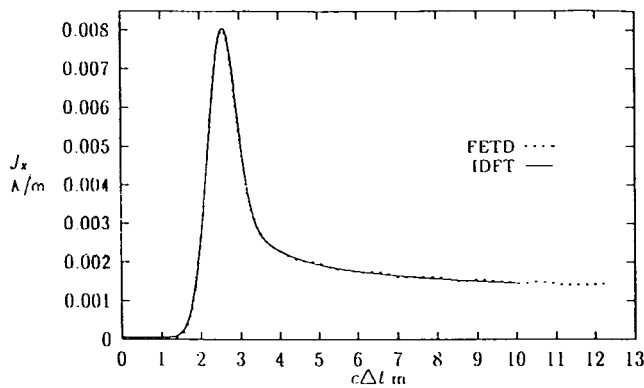


Fig. 7. Induced current on the half cylinder at  $(0.5, 0.0)$ . Outer boundary— $0.2$  m away.

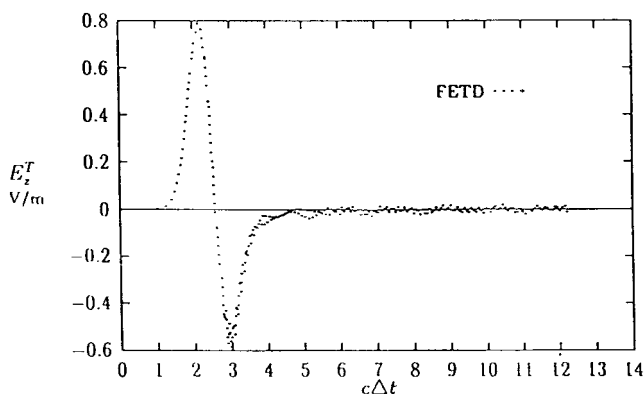


Fig. 8. Total electric field on the terminating surface at a point  $(0.7, 0.0)$ .

The total electric field for a node residing on the terminating surface has been plotted in Fig. 6. We can clearly observe that the incident wave passes through the node and, after reflection from the conducting surface, reaches its negative maximum around 3 before coming back to zero.

### C. Half Cylinder

As a final example, consider the scattering from a half-cylinder of diameter  $1.0$  m. We have employed four layers of finite elements to discretize the space between the fictitious surface and scatterer. The terminating surface is conformal to the body and is only  $0.2$  m away from the surface of the conductor. The incident field in this case is coming from  $\theta = 90^\circ$ . Again, we have used the total field formulation for this problem. Electric-field values are found out for 180 free nodes at every time step. The tangential electric field on the scatterer, formed by 50 fixed nodes, is zero for the total field formulation. As before, the time-stepping procedure starts by assuming  $\bar{E}_i$  on the outside boundary, which is comprised of 60 fixed nodes. The finite-element matrix of (21) is solved for the unknown free nodes. The normal derivative of the electric field is computed, which gives the current distribution over a particular segment at a time instant through (13). With these known currents, at every time step the radiation condition on the outside boundary is employed through Green's-function integral equation (5). We have used the same width and delay

of the Gaussian pulse as employed in previous examples. The time step chosen is  $\frac{1}{21}$  nm.

The induced surface current for a node residing on the  $y$ -axis with time progression is plotted in Fig. 7, and is marked as FETD. As expected, the induced current reaches its peak when the peak of the incident wave hits the particular node. For the MOM, we have used inverse discrete Fourier-transformed frequency-domain MOM results to compare the result from this method. We have used 256 equally spaced frequency samples to get the inverse transform. 52 subsections are chosen to calculate induced current using the MOM. As before, pulse basis functions and point-matching testing procedure are used to evaluate the current on the conductor. This result is marked as IDFT in Fig. 7. The total electric field on a node residing on the terminating surface is plotted in Fig. 8, and it decays to zero.

It has been our experience that placing the boundary too close to the body or keeping it too far away introduces different kinds of problems. While placing it too close, we observed small ripples in the late time solution even though they do not produce any kind of instability. While keeping it very far away from the body, and using very few layers of finite elements between the body and transmitting surface, we introduce errors in the computation of the normal derivative of the electric field. This may produce an erroneous induced current at every time step, which in turn computes an incorrect scattered fields at the terminating surface and, hence, inappropriate radiation condition for the surface.

## VI. CONCLUSION

A hybrid method is presented for the solution of the wave equation in two dimensions for open-region TM scattering problems using time-domain analysis. The results are in good agreement with the IDFT solution of the MOM (transformed to time domain) from frequency domain. The implicit integration scheme of the Newmark method makes the finite-element matrix equation to be unconditionally stable systems for some particular values of  $\alpha$  and  $\delta$ . This paper provides a method for using finite-element techniques for solving transient problems in open regions.

## REFERENCES

- [1] T. Roy, T. K. Sarkar, A. R. Djordjevic, and M. Salazar, "A hybrid method for terminating the finite element mesh (electrostatic case)," *Microwave Opt. Technol. Lett.*, vol. 8, no. 6, pp. 282–287, Apr. 1995.
- [2] ———, "A hybrid method for solution of scattering by conducting cylinder (TM case)," *IEEE Trans. Microwave Theory Tech.*, vol. 44, pp. 2145–2151, Dec. 1996.
- [3] K. S. Yee, "Numerical solution of initial boundary value problems involving Maxwell equation in isotropic media," *IEEE Trans. Antennas Propagat.*, vol. AP-14, pp. 302–107, May 1966.
- [4] C. L. Bennett and W. L. Weeks, "Transient scattering from conducting cylinders," *IEEE Trans. Antennas Propagat.*, vol. AP-18, pp. 627–633, Sept. 1970.
- [5] A. G. Tijhuis, "Toward a stable marching-on-in-time method for two-dimensional transient electromagnetic scattering problems," *Radio Sci.*, vol. 19, no. 5, pp. 1311–1317, Sept. 1984.
- [6] A. Sadigh and E. Arvas, "Treating instabilities in marching-on-in-time method from a different perspective," *IEEE Trans. Antennas Propagat.*, vol. 41, pp. 1695–1702, Dec. 1993.

- [7] D. A. Vechinski, "Direct time-domain analysis of arbitrary shaped conducting or dielectric structures using patch modeling techniques," Ph.D. dissertation, Dept. Elect. Eng., Auburn Univ., Auburn, AL, 1992.
- [8] B. P. Rynne and P. D. Smith, "Stability of time marching algorithms for the electric field equation," *J. Electromagn. Waves Applicat.*, vol. 4, pp. 1181-1205, 1990.
- [9] B. P. Rynne, "Time domain scattering from arbitrary surfaces using the electric field equation," *J. Electromagn. Waves Applicat.*, vol. 8, pp. 85-114, 1994.
- [10] S. Barkeshli, H. A. Sabbagh, D. J. Radecki, and M. Melton, "A novel implicit time-domain boundary integral/finite-element algorithm for computing transient electromagnetic field coupling to a metallic enclosure," *IEEE Trans. Antennas Propagat.*, vol. 40, pp. 1155-1164, Oct. 1992.
- [11] S. D. Gedney and U. Navsariwala, "An unconditionally stable finite element time-domain solution of the vector wave equation," *IEEE Microwave Guided Wave Lett.*, vol. 5, pp. 332-334, Oct. 1995.
- [12] J. Jin, *Finite Element Method in Electromagnetics*. New York: Wiley, 1993.
- [13] K. J. Bathe, *Finite Element Procedures in Engineering Analysis*. Englewood Cliffs, NJ: Prentice-Hall, 1982.
- [14] R. F. Harrington, *Field Computation by Moment Methods*. New York: Macmillan, 1968.

**Tanmoy Roy** received the B.Tech. degree from the Indian Institute of Technology, Kharapur, India, in 1990, and the M.S. and Ph.D. degrees in electrical engineering from Syracuse University, Syracuse, NY, in 1995 and 1996, respectively.

From 1990 to 1991, he was a Software Consultant for Tata Consultancy Services, India. IN 1994 and 1995, he was a summer Intern at Schlumberger-Doll Research, Ridgefield, CT. He is currently with Sun Microsystems, Palo Alto, CA. His research interests deal with finite-element techniques.



**Tapan K. Sarkar** (S'69-M'76-SM'81-F'92) received the B.Tech. degree from the Indian Institute of Technology, Kharapur, India, the M.Sc.E. degree from the University of New Brunswick, Fredericton, Canada, in 1969, and the M.S. and Ph.D. degrees from Syracuse University, Syracuse, NY, in 1971 and 1975, respectively.

From 1975 to 1976, he was with the TACO Division, General Instruments Corporation. From 1976 to 1985, he was with the Rochester Institute of Technology, Rochester, NY. From 1977 to 1978, he

was a Research Fellow at the Gordon McKay Laboratory, Harvard University, Cambridge, MA. He is currently a Professor in the Department of Electrical and Computer Engineering, Syracuse University. He has authored or co-authored over 180 journal articles and has written chapters in eight books. His current research interests deal with numerical solutions of operator equations arising in electromagnetics and signal processing with application to system design.

Dr. Sarkar is a Registered Professional Engineer in the State of New York. He is a member of Sigma Xi and the International Union of Radio Science Commissions A and B. He was an associate editor for feature articles of the *IEEE Antennas and Propagation Society Newsletter*. He was the technical program chairman for the 1988 IEEE AP-S International Symposium and URSI Radio Science Meeting, and has been appointed U.S. research council representative to many URSI General Assemblies. He is the chairman of the Intercommission Working Group of International URSI on Time-Domain Metrology. He received one of the "Best Solution" Awards in 1977, presented at the Rome Air Development Center (RADC) Spectral Estimation Workshop, the Best Paper Award of the IEEE TRANSACTIONS ON ELECTROMAGNETIC COMPATIBILITY in 1979, and a Best Paper Award at the 1997 National Radar Conference (NATRAD'97).



**Antonije R. Djordjevic** was born in Belgrade, Yugoslavia, on April 28, 1952. He received the B.Sc., M.Sc., and D.Sc. degree from the School of Electrical Engineering, University of Belgrade, Belgrade, Yugoslavia, in 1975, 1977, and 1979, respectively.

In 1975, he joined the School of Electrical Engineering, University of Belgrade, as a Teaching Assistant. In 1982, he was promoted to an Assistant Professor, in 1988, to an Associate Professor, and since 1992, he has been a Professor. In 1983, he was a Visiting Associate Professor at the Rochester Institute of Technology, Rochester, NY. Since 1992, he also has been an Adjunct Associate Professor at Syracuse University, Syracuse, NY. His main field of interest is numerical electromagnetics, in particular, applied to multiconductor transmission lines, wire and surface antennas, and electromagnetic-compatibility problems.

Dr. Djordjevic is an corresponding member of the Serbian Academy of Sciences and Arts.



**Magdalena Salazar-Palma** (M'89) was born in Granada, Spain. She received the *Ingeniero de Telecomunicación* and Ph.D. degrees from the Universidad Politécnica de Madrid, Madrid, Spain.

She is currently a Professor Titular in the Departamento de Senales, Sistemas y Radiocomunicaciones, ETSI Telecomunicacion, Universidad Politecnica de Madrid. She has taught courses on electromagnetic field theory, microwave and antenna theory, circuit networks and filter theory, analog and digital communication systems theory, numerical methods for electromagnetic-field problems, as well as related laboratories. She has developed her research with the Grupo de Microondas y Radar in the areas of electromagnetic-field theory, computational and numerical methods for microwave structures, passive components, and antenna analysis, the design, simulation, optimization, implementation, and measurements of hybrid and monolithic microwave integrated circuits, and network and filter theory and design. She has authored 10 contributions for chapters and articles in books, 15 papers in international journals, and 75 papers in international conferences, symposiums, and workshops, plus a number of national publications and reports. She has delivered a number of invited presentations, lectures, and seminars. She has lectured in several short courses. She has participated in 19 projects and contracts financed by international, European, and national institutions and companies. She has been a member of the Technical Programme Committee of several international symposiums, and has acted as reviewer for different international scientific journals, symposiums, and editorial companies. She has assisted the Comisión Interministerial de Ciencia y Tecnología (National Board of Reserach) in the evaluation of projects. She has also served in several evaluation panels of the Commission of the European Communities. She is currently a Topical Editor for the disk of references of the triennial *Review of Radio Science*. She is a member of the editorial board of two scientific journals.

Dr. Salazar-Palma has served as vice-chairman and chairman of the IEEE Microwave Theory and Techniques Society and IEEE Antennas and Propagation Society Spanish joint chapter, and is currently serving as chairman of the Spain section of the IEEE. She has received two individual research awards from national institutions.